NeuroImage: Clinical 29 (2021) 102528

Contents lists available at ScienceDirect

NeuroImage: Clinical

journal homepage: www.elsevier.com/locate/ynicl

The cingulum in very preterm infants relates to language and social-emotional impairment at 2 years of term-equivalent age

Hyun Ju Lee [a,e,1], Hyeokjin Kwon [b,1], Johanna Inhyang Kim [c,e], Joo Young Lee [a], Ji Young Lee [d], SungKyu Bang [b], Jong-Min Lee [f,*]

[a] Department of Pediatrics, Hanyang University College of Medicine, Seoul, South Korea
[b] Department of Electronic Engineering, Hanyang University, Seoul, South Korea
[c] Department of Psychiatry, Hanyang University, Seoul, South Korea
[d] Department of Radiology, Hanyang University College of Medicine, Seoul, South Korea
[e] Division of Neonatology and Developmental Medicine, Seoul Hanyang University Hospital, Seoul, South Korea
[f] Department of Biomedical Engineering, Hanyang University, Seoul, South Korea

ARTICLE INFO

Keywords:
Very preterm infants
Diffusion tensor imaging (DTI)
White matter (WM)
Elastic net logistic regression model
Bayley scales

ABSTRACT

Background: Relative to full-term infants, very preterm infants exhibit disrupted white matter (WM) maturation and problems related to development, including motor, cognitive, social-emotional, and receptive and expressive language processing.
Objective: The present study aimed to determine whether regional abnormalities in the WM microstructure of very preterm infants, as defined relative to those of full-term infants at a near-term age, are associated with neurodevelopmental outcomes at the age of 18–22 months.
Methods: We prospectively enrolled 89 very preterm infants (birth weight < 1500 g) and 43 normal full-term control infants born between 2016 and 2018. All infants underwent a structural brain magnetic resonance imaging scan at near-term age. The diffusion tensor imaging (DTI) metrics of the whole-brain WM tracts were extracted based on the neonatal probabilistic WM pathway. The elastic net logistic regression model was used to identify altered WM tracts in the preterm brain. We evaluated the associations between the altered WM microstructure at near-term age and motor, cognitive, social-emotional, and receptive and expressive language developments at 18–22 months of age, as measured using the Bayley Scales of Infant Development, Third Edition.
Results: We found that the elastic net logistic regression model could classify preterm and full-term neonates with an accuracy of 87.9% (corrected $p < 0.008$) using the DTI metrics in the pathway of interest with a 10% threshold level. The fractional anisotropy (FA) values of the body and splenium of the corpus callosum, middle cerebellar peduncle, left and right uncinate fasciculi, and right portion of the pathway between the premotor and primary motor cortices (premotor-PMC), as well as the mean axial diffusivity (AD) values of the left cingulum, were identified as contributive features for classification. Increased adjusted AD values in the left cingulum pathway were significantly correlated with language scores after false discovery rate (FDR) correction ($r = 0.217$, $p = 0.043$). The expressive language and social-emotional composite scores showed a significant positive correlation with the AD values in the left cingulum pathway ($r = 0.226$ [$p = 0.036$] and $r = 0.31$ [$p = 0.003$], respectively) after FDR correction.
Conclusion: Our approach suggests that the cingulum pathways of very preterm infants differ from those of full-term infants and significantly contribute to the prediction of the subsequent development of the language and social-emotional domains. This finding could improve our understanding of how specific neural substrates

Abbreviations: WM, White matter; DTI, diffusion tensor imaging; FA, fractional anisotropy; MD, mean diffusivity; AD, axial diffusivity; RD, radial diffusivity; FDR, false discovery rate; TBSS, tract-based spatial statistics; ROI, region of interest; TBM, tensor-based morphometry; MVPA, multivariate pattern analysis; SVM, support vector machine; LASSO, least absolute shrinkage and selection operator; RF, random forest; MRI, magnetic resonance imaging; PMA, postmenstrual age; GA, gestational age; IVH, intra-ventricular hemorrhage; BSID-III, Bayley Scales of Infant and Toddler Development, Third Edition; SD, standard deviation; MCP, middle cerebellar peduncle; SLF, superior longitudinal fasciculus; AF, arcuate fasciculus; premotor-PMC, the pathway between the premotor and primary motor cortices; CC, corpus callosum; ANTs, advanced normalization tools; FoV, field of view.

* Corresponding author at: Department of Biomedical Engineering, Hanyang University, 17 Haengdang-dong, Seongdong-gu, Seoul 133-792, South Korea
E-mail address: ljm@hanyang.ac.kr (J.-M. Lee).

[1] Hyun Ju Lee and Hyeokjin Kwon contributed equally to this work. Co-first authorship should be mentioned in the present part.

https://doi.org/10.1016/j.nicl.2020.102528
Received 26 June 2020; Received in revised form 15 October 2020; Accepted 4 December 2020
Available online 8 December 2020

influence neurodevelopment at later ages, and individual risk prediction, thus helping to inform early intervention strategies that address developmental delay.

1. Introduction

Remarkable advances in postnatal care and technology have improved the survival rates for preterm infants. Previous studies have reported variable results while observing the neurodevelopmental trajectories of children born very or extremely preterm from preschool to early adulthood (Cheong et al., 2017; Linsell et al., 2018; Twilhaar et al., 2018). Half of all children born very preterm develop cognitive delay and language impairment that detrimentally impact their academic performance and social skills (Erdei et al., 2020; Linsell et al., 2015; Serenius et al., 2016). A recent study observed that 34–49% of children born very preterm showed mild cognitive delay by school age, while 10–16% developed severe intellectual impairment (Erdei et al., 2020). Although the early identification of children with mild cognitive delay is challenging at younger ages, early intervention may help to mitigate adverse consequences to their mental health and long-term educational achievement.

Notably, one of every three very preterm infants has an elevated risk of developing language impairment before the age of 3, indicating that very preterm infants are affected by subtle language barriers even before their cognitive function fully develops during adolescence (Sansavini et al., 2010). The aberrant cognitive development observed in preterm infants may be related to the widespread regional differences in diffusion tensor imaging (DTI) parameters between preterm infants and their full-term counterparts at near-term age during normal brain maturation (Li et al., 2015; Rogers et al., 2018). Further, a recent systematic review found that abnormal developmental trajectories of specific white matter (WM) pathways correlate with the language scores of school-aged preterm children (Stipdonk et al., 2018). Preterm birth induces both immediate and long-lasting changes in language-related pathways and networks observable at the neonatal period, adolescence, and adulthood (Kwon et al., 2016). The early identification of language deficits mediating cognitive impairment is necessary for the timely execution of targeted interventions during periods of neuroplasticity before the age of 3 years.

DTI is a noninvasive tool with a high sensitivity to changes in myelination, and axonal density and diameter, that can be used to investigate the pathophysiology underlying unfavorable neurodevelopmental alterations in the preterm brain (Rogers et al., 2016). While previous reports of altered WM in preterm children have been obtained using univariate analytical methods with high exploratory power – e.g., region of interest (ROI)-based analysis (Caldinelli et al., 2017; Dodson et al., 2017; Murray et al., 2016), tract-based spatial statistics (TBSS) (Coker-Bolt et al., 2016; Collins et al., 2019; Hollund et al., 2018; Jurcoane et al., 2016; Murner-Lavanchy et al., 2018), and tensor-based morphometry (TBM) (Rajagopalan et al., 2017) – these methods may be too conservative to detect subtle, spatially distributed differences because they require corrections for multiple comparisons to control the expected false discovery rate (FDR) (Ecker et al., 2010b). By contrast, a multivariate pattern analysis (MVPA) (e.g., support vector machine (SVM) and logistic regression models) accounts for interregional correlations and features increased sensitivity to abnormalities in neural systems (Ecker et al., 2010b; Li et al., 2014; Little and Beaulieu, 2019; Schadl et al., 2018). MVPA uses multivariate features from neuroimaging data to classify individual observations into different groups and thus reveals the contributing spatial and/or temporal patterns associated with the categories (Lao et al., 2004). Further, compared with univariate statistical analysis, MVPA has enhanced clinical applicability and provides insights regarding individual-level rather than group-level inferences (Pereira et al., 2009).

MVPA has thus garnered increasing interest as an alternative method for the analysis of neuroimaging data. In recent years, MVPA has been used to predict cognition at the age of 2 years from DTI findings (Girault et al., 2019), identify WM impairments in patients with HIV (Tang et al., 2017), evaluate the predictive value of structural magnetic resonance imaging (MRI) in autism spectrum disorders (ASD) (Ecker et al., 2010b), and delineate sex-related neuroanatomical differences (Baldinger-Melich et al., 2019). Ecker et al. successfully differentiated individuals with ASD from healthy controls using linear SVM, despite the method's limitations regarding the resolution of noisy neuroimaging data (Ecker et al., 2010b; Liu et al., 2012). Schadl et al. accurately predicted cognitive and motor impairments at age 2 from regional WM microstructures, from near-term DTI data using logistic regression learning approaches and exhaustive feature selection in preterm infants (Schadl et al., 2018). Relative to penalized logistic regression models, logistic regression models can increase the variance of the prediction more easily when changing the training data set, and are more prone to overfitting. Hence, $\ell 1$ (Tibshirani, 1996) and $\ell 2$ (Hoerl and Kennard, 1970) penalties on regression parameters were introduced in the regression model to enforce sparse solutions by shrinking the parameters (Tibshirani, 1996; Zou and Hastie, 2005). For example, the ridge regression was designed by using the $\ell 2$-norm of the model parameters to mitigate the multicollinearity of the explanatory variables, which is usually considered independent in the regression analysis (Hoerl and Kennard, 1970; Kibria, 2003). Similarly, instead of using the quadratic part of the coefficients, the least absolute shrinkage and selection operator (LASSO) regression model proposes a modified objective function for the minimization of the ordinary sum of squares, subject to regularized $\ell 1$-norm of the regression coefficients (Tibshirani, 1996). The use of $\ell 1$-regularization forces the model to find coefficients with a value of exactly 0 and thus allows for variable selection (Ryali et al., 2010; Vounou et al., 2010). However, while these regression penalty techniques are powerful, they are limited by featuring unstable solution paths for LASSO and high sensitivity to atypical samples for the ridge model (Yang and Zou, 2013). On the other hand, Zou and Hastie et al. established an elastic net regression model by introducing a combination of $\ell 1$- and $\ell 2$-norm penalization, and showed that it can overcome the restriction of the LASSO and ridge (Zou and Hastie, 2005); the elastic net logistic regression model significantly outperforms ordinary least-square logistic regression in the classification of cancer with high-dimensional genetic data (Algamal and Lee, 2015), identification of biomarkers for mild cognitive impairment and Alzheimer's disease (Shen et al., 2011), and classification of multilabel image (Li et al., 2016).

Little is known about DTI biomarkers in the preterm brain that are predictive of future neurodevelopmental outcomes and emergent language abilities. Furthermore, despite the significance of the critical period of brain development around near-term age, our understanding of the role of atypical brain development at this age in determining subsequent neurodevelopmental outcomes remains incomplete. Stipdonk et al. implicated several microstructural brain areas – not just a single region – in the non-normative development of language skills in school-aged preterm children (Stipdonk et al., 2018). Recent evidence suggests that the aberrant development of WM substrates in very preterm infants preceded the manifestation of cognitive delay and language deficits; however, little is known about DTI biomarker using the MVPA from a global WM component to optimize predictive ability as early as near-term age.

We hypothesized that the global WM pattern at birth in preterm individuals would inform the prediction of emergent neurodevelopmental outcomes at the age of 2 years. We further evaluated the usefulness of neuroimaging biomarkers in early brain organization to

predict subsequent neurodevelopmental outcomes beyond 2 years of age. We applied the elastic net logistic regression model to the DTI metrics of fractional anisotropy (FA), mean diffusivity (MD), axial diffusivity (AD), and radial diffusivity (RD) to classify the WM tracts in preterm and full-term infants. We then selected the most contributive features based on the parameters of the classification model and defined them as altered WM microstructures. Finally, we performed a partial correlation analysis to investigate the relationship between the identified regional abnormalities in the WM microstructures and subsequent neurodevelopmental outcomes at 18–22 months in very preterm children.

2. Materials and methods

2.1. Subjects and clinical assessment

The present prospective, longitudinal study analyzed data obtained from a cohort of very preterm infants with birth weights of <1.5 kg. All infants were recruited from the Level 3 Neonatal Intensive Care Unit of Hanyang University Hospital between February 2016 and October 2018 and attended follow-up at the same institution. The following inclusion criteria were used for enrollment: (1) born before 32 weeks of gestation with a birth weight of <1.5 kg; (2) available MRI-DTI data obtained at a near-term age without focal abnormalities (postmenstrual age [PMA], 37–41 weeks); and (3) no evidence of intra-ventricular hemorrhage (IVH) or brain injury, as diagnosed with cranial ultrasonography or MRI. Infants with chromosomal abnormalities, proven congenital infections, congenital anomalies, or intrauterine growth retardation were excluded.

Twenty-nine infants were excluded from the total cohort of 118 eligible infants: one was diagnosed with 9q34 duplication syndrome after enrollment, one failed to obtain parental consent, one transferred to another hospital before reaching near-term age, five died during neonatal intensive care, six showed motion artifacts on MRI data, and 15 exhibited brain abnormalities indicative of IVH, post-hemorrhagic hydrocephalus, or cystic periventricular leukomalacia. Hence, 89 very preterm infants were included in the study. The following prenatal and neonatal data were prospectively recorded: gestational age (GA), birth weight, PMA at imaging, sex, and maternal age and education. We also prospectively enrolled 43 full-term singleton control infants (38–42 weeks of gestation) with normal MRI findings from the Hanyang Inclusive Clinic for Developmental Disorders, Hanyang University College of Medicine. Exclusion criteria for full-term infants were chromosomal abnormalities, congenital infections, acidosis on arterial blood gas assessed during the first hour of life, and evidence of seizure events in the course of neonatal care. The parents of all the infants provided informed consent for their children's participation in the study prior to its commencement. The institutional review board (IRB No. 2017-04-004) of Hanyang University Hospital approved our study protocol and scanning procedures. This study was conducted in accordance with the principles of the Declaration of Helsinki.

2.2. Neurodevelopmental assessment

The neurodevelopment of preterm infants and full-term controls was prospectively assessed with the Bayley Scales of Infant and Toddler Development, Third Edition (BSID-III) at 18–22 months of corrected age adjusted for prematurity (i.e., the age at which the preterm infant would have been born on his or her due date) at the Hanyang Inclusive Clinic for Developmental Disorders, Hanyang University College of Medicine (Bayley, 2009). Routine clinical examinations and structured neurodevelopmental assessments were completed by an experienced developmental pediatrician, a physiotherapist, and a neonatologist at 18–22 months of corrected age, according to the follow-up program. Outcome measures included cognition, language, motor, and social-emotional composite scores. Language scores included receptive and expressive sub-scaled scores. Assessments of the infants' cognitive, language, and motor domains were performed with the children, while those of the social-emotional domains were informed by the primary caregiver's responses to a questionnaire in the BSID-III. The normative mean (standard deviation [SD]) for each outcome score was 100, and scores of <85 (1 SD below average) were considered to indicate neurodevelopmental delay. Composite or scaled scores of the BSID-III were based on the child's adjusted age at the time of evaluation. Children were classified as having developmental delay if their BSID-III composite scores fell <1 SD below the mean BSID-III cognitive, language, motor, and social-emotional scale scores at 18–22 months of adjusted age.

2.3. Magnetic resonance imaging

MRI brain scans were obtained during natural sleep at near-term age between the PMA of 35 and 42 weeks in preterm infants and within one month of birth (PMA, 37–42 weeks) in full-term control infants using a 3.0-T MRI scanner (Philips real-time compact magnet 3.0-T MRI system; Achieva 3.0 T X-Series) with a 16-channel SENSE head coil. To ensure that the neonates were sleeping during the scan, they were fed beforehand and wrapped in a blanket. Subjects were placed on cushions placed on top of the radiofrequency coil. Oxygen saturation (through pulse oximetry), respiratory rate, and heart rate were monitored. A trained pediatrician attended the MRI examinations. T1-weighted images were acquired with Turbo Field Echo sequences and the following parameters: TR = 8.1 ms, TE = 3.7 ms, field of view (FoV) = 180 × 180 mm, spatial resolution = 0.6 × 0.6 × 1 mm, and slice thickness = 1.0 mm. Structural T2-weighted images were obtained to exclude WM abnormalities. The Turbo Spin Echo T2 scan imaging parameters were as follows: TR = 4800 ms, TE = 90 ms, FoV = 180 × 180 mm, spatial resolution = 0.5 × 0.5 × 4 mm, and slice thickness = 4.0 mm. Radiological evaluation was performed by an experienced pediatric neuroradiologist who was blinded to all other data. DTI was acquired using a single-shot spin-echo planar sequence with a SENSE factor of 2 and an echo planar imaging factor of 51 (TR = 5500 ms, TE = 89 ms, FoV = 150 × 150 mm, resolution = 2 × 2 × 2 mm, slice thickness = 2.0 mm). The slice orientation was axial, and parallel to the anterior-posterior commissure line. A total of 40–50 slices covered the entire hemisphere and brainstem. Diffusivities were measured along 15 directions using an electrostatic gradient model (b = 800).

2.4. DTI preprocessing

Diffusion-weighted images were processed using FMRIB's Software Library (http://www.fmrib.ox.ac.uk/fsl). The skull and non-brain tissue were removed from the non-diffusion-weighted volume (b0 volume) using the Brain Extraction Tool. The MR susceptibility-induced field, eddy current distortions, and motion artifacts were corrected with outlier replacement using the eddy tool. The bias field estimation was performed for b0 volume to avoid low-frequency intensity inhomogeneity and its influence on diffusion data. The estimated bias field was applied to all diffusion-weighted volumes using Advanced Normalization Tools (ANTs) (Tustison et al., 2010). Subsequently, the diffusion tensor model was used for calculations in each voxel, using a simple least-square fit of the model. FA, MD, AD, and RD were also calculated from the tensor eigenvalues, which describe the three major diffusion directions. Finally, the John Hopkins University (JHU) neonatal probabilistic WM pathway atlas was aligned to the FA image of the native diffusion space using a nonlinear symmetric normalization algorithm in ANTs to calculate the average FA, MD, AD, and RD values for each pathway (Avants et al., 2008; Oishi et al., 2011). The atlas provided a total of 27 major fibers on the population-averaged neonatal template. With no prior knowledge, all regions were used for the calculation of DTI indices, except for corpus callosum (CC), which overlapped with segmented regions of itself (the genu of the CC, the body of the CC, and the splenium of the CC). The DTI measures of each

pathway were adjusted for PMA at scan and maternal education using multiple linear regression models. The atlas threshold was set at a range of levels (10%, 30%, 50%, and 70%) prior to aligning the FA image. Additionally, visual inspection of the registration quality was performed for each individual FA image to validate the analysis (Supplementary Fig. 1 shows that the aligned pathways were correctly overlaid onto the representative FA map for each group).

2.5. Framework for multivariate pattern analysis in preterm and full-term infants

The framework of the analysis in this study consisted of group classification, identification of the most contributive features, and correlation analysis (Fig. 1). We used the elastic net logistic regression model with 10-fold cross-validation to classify preterm and full-term individuals. We calculated the classification accuracy, sensitivity, specificity, f1 score, and positive predicted value, and subsequently identified the highly contributive pathways and DTI metrics. We also showed the potential power of the elastic net regression classification model in comparison with other models such as LASSO penalized logistic regression, linear SVM, and random forest (RF). Finally, we examined partial correlations between the DTI metrics of the specified pathways and neurodevelopmental outcomes in the subjects of each group.

2.6. Group-classification models

We used the elastic net logistic regression model to classify subjects using the DTI metrics of all WM pathways. The elastic net logistic regression model is capable of selecting regressors with sparsity parameters, because highly correlated and redundant features can result in overfitting and can increase the variance of the classification model. The model equation is as follows:

$$\min_{\boldsymbol{w},w_0}(1-\rho)(\boldsymbol{w}^T\boldsymbol{w}/2)+\rho\|\boldsymbol{w}\|_1+C\sum_{i=1}^{n}\log(\exp(-\boldsymbol{y}_i(\boldsymbol{X}_i{}^T\boldsymbol{w}+w_0))+1) \quad (1)$$

where $\boldsymbol{y}$ is a vector of the size n × 1 containing the group label (n = 132; sample was labeled "1″ for preterm and "-1" for full-term) of the subjects, $\boldsymbol{X}$ is a matrix of the size n × 104 containing the DTI metrics calculated from the 26 WM pathway regions, C is the inverse of the regularization strength, and ρ controls the balance of the ℓ1 and ℓ2 regularizations. The 10-fold cross-validation and grid search strategy was performed to choose the optimal regularization parameters C and ρ (Casanova et al., 2011; Stolicyn et al., 2020). The mean misclassification rate for each pair of C and ρ was calculated in the training set over a range of different values between 0 and 1 with increments of 0.01 (C, total of 100 values) and 0.05 (ρ, total of 20 values). The "optimal" hyperparameter pair with the lowest mean misclassification rate was then chosen for each fold. Similarly, the 10-fold cross-validation was performed and grid-search framework was employed to choose the optimal regularization parameter C (ρ was set to 1 in Eq. (1)) when using the LASSO logistic regression model.

An SVM with a linear kernel was also used to perform group classification. The optimal discriminative hyperplane was established in the feature space using the nearest samples (support vectors) in the model. In the soft-margin SVM model, the condition for the solution of the hyperplane could be relaxed by introducing a misclassification error. Parameter C controls the tradeoff between margin optimization and the allowance for misclassifications. Similarly, the 10-fold cross-validation and grid search was performed over a range of different C values to determine an optimal parameter for each training set. RF is a bootstrap aggregation (bagging) classifier consisting of multiple independent decision trees. Typically, each tree is trained using random feature selection, and the final output for a sample is obtained by conducting majority voting. The optimal number of trees that minimize the out-of-

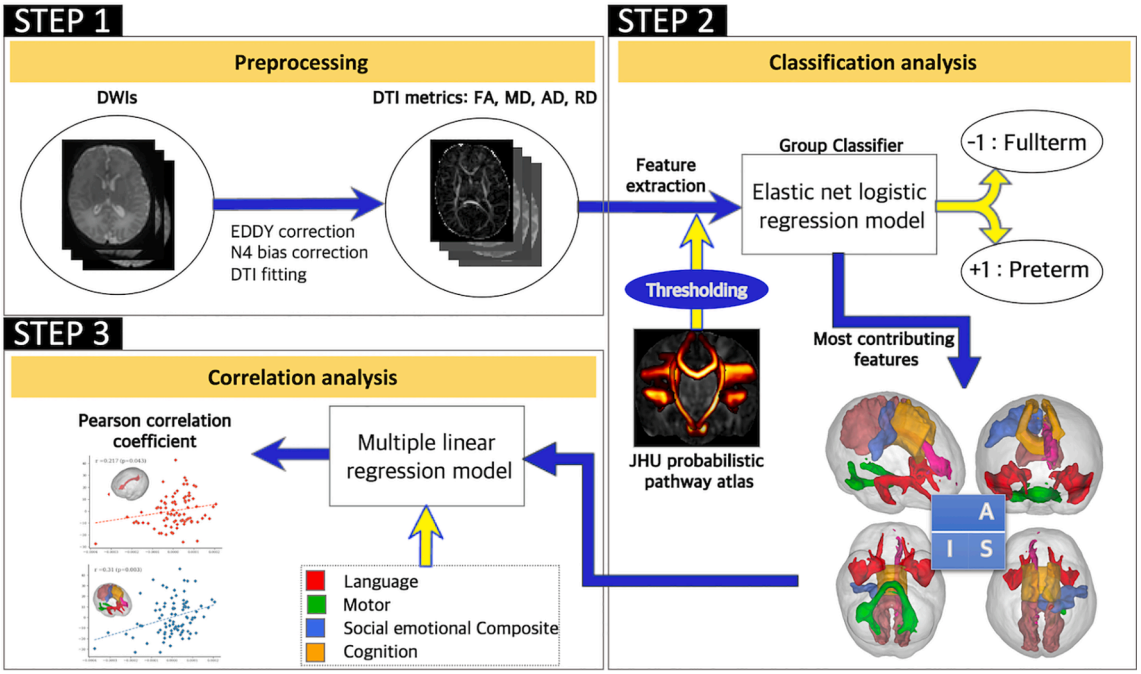

Fig. 1. Analysis flowchart. (STEP1) MR susceptibility-induced field, eddy current distortions, and motion artifacts of the individual diffusion weighted images were corrected, and diffusion tensor imaging metrics (FA, MD, AD, and RD map) were calculated by using the voxel-wise diffusion tensor modeling. (STEP2) After thresholding the John Hopkins University probabilistic white-matter pathway atlas, features were extracted by calculating the mean DTI metrics of the WM pathway regions. Using the elastic net logistic regression model, individuals were classified into either the preterm or full-term group. The most contributive features were then identified using parameters of the trained elastic net logistic regression model. (STEP3) Finally, partial correlation analysis was performed between the selected features and neurodevelopmental domains after removing the covariate effects with the multiple linear regression model. MR, magnetic resonance; FA, fractional anisotropy; MD, mean diffusivity; AD, axial diffusivity; RD, radial diffusivity; DTI, diffusion tensor imagin; WM, white matter;

bag error of the training dataset was chosen for each fold. Finally, the rate for random feature selection was empirically set to one-third of the number of features. All classifications were performed using the scikit-learn package version 0.22.1 (Pedregosa et al., 2011).

2.7. Model evaluation and identification of the most contributing features

Permutation tests were conducted to verify the statistical significance of the classifications (Nichols and Holmes, 2002; Ojala and Garriga, 2010). We randomly permuted the group labels 500 times, and performed the 10-fold cross-validation based on the permutated samples to calculate the accuracy of each permutation. Defined at a confidence level of 0.05, model significance was calculated by dividing the number of times the model achieved a higher accuracy than that of the true labels plus one by 501 (i.e., the number of all tests including the original one). All p-values were FDR corrected for multiple comparisons (four comparisons, effective $p < 0.0125$).

Consistent with the methods of previous studies (Ecker et al., 2010a, 2010b; Mourao-Miranda et al., 2005), we calculated the distance from the baseline for the odds ratios of the 104 features and selected the features with absolute values of ≥30% of the maximum and minimum cases. Similarly, 30% of the features with the highest weight/importance were selected for SVM and RF.

2.8. Correlation between DTI measures and clinical neurodevelopmental outcomes

Within-group partial correlation analysis was performed to examine the association between the selected features and neurodevelopmental outcomes. For each DTI metric and neurodevelopmental outcome, residual components were calculated for the PMA at scan and maternal education effects, using the multiple linear regression model prior to correlation analysis. Pearson's correlation coefficient was calculated using the statsmodels package version 0.17.1 (Seabold and Perktold, 2010). All p-values were FDR-corrected for multiple comparisons.

3. Results

3.1. Clinical characteristics

The present study recruited 89 preterm and 43 full-term infants (Table 1 and Table 2). Of the 89 preterm infants, 88 attended follow-ups at 18–22 months: one was excluded due to lack of follow-up. Of the 43 full-term infants, 38 attended follow-ups at 18–22 months: three withdrew from the study, and we were unable to contact the parents of two. Of the 126 infants who completed the BSID-III, there were fewer males than females (54:72, 57.1%). There were no significant differences between males and females in neurodevelopmental outcomes, including cognitive (97.41 ± 12.39 vs 98.83 ± 12.25, $p = 0.521$), language (91.26 ± 12.91 vs 92.11 ± 13.54, $p = 0.722$), motor (99.83 ± 17.41 vs 99.60 ± 15.41, $p = 0.936$), and social-emotional (102.78 ± 17.42 vs 100.28 ± 16.11, $p = 0.407$) outcomes. Among the preterm infants, males had lower cognitive (95.55 ± 13.36 vs. 98.75 ± 12.24, $p = 0.146$), language (86.33 ± 12.39 vs 91.25 ± 13.78, $p = 0.096$), motor (94.15 ± 17.64 vs 97.69 ± 15.51, $p = 0.328$), and social-emotional scores (96.52 ± 16.12 vs 99.18 ± 16.85, $p = 0.467$); however, these differences were nonsignificant. While the preterm group scored lower on language assessments than the control group, there were no meaningful differences between the two groups (97.17 ± 12.76 vs. 100.66 ± 10.85, $p = 0.144$). Further, while the receptive scaled score (8.74 ± 2.44 vs. 9.42 ± 1.61, $p = 0.117$) in the language domain was comparable between the groups, the expressive scaled score (8.20 ± 2.53 vs. 9.89 ± 1.54, $p < 0.001$) in the same domain was remarkably lower in very preterm infants. Preterm infants had significantly lower mean composite scores in the motor (96.36 ± 16.33 vs. 107.42 ± 13.25, $p = 0.001$) and social-emotional (98.18 ± 16.54 vs. 108.68 ± 14.69, $p = 0.001$) domains than the full-term infants. The incidence of infants with language (40.9% vs. 13.2%, $p = 0.002$), motor (17% vs. 0%, $p = 0.005$), and social-emotional (15.9% vs. 0%, $p = 0.010$) delays was significantly higher among the very preterm infants than among the full-term infants.

Table 1
Characteristics of preterm and term infants.

Variables	Preterm (n = 89)	Term (n = 43)	P-value
Infant characteristics			
Gestational age, wk	28.65 ± 2.63	38.21 ± 1.20	<0.001
Birth weight, g	1157.20 ± 262.39	3103.42 ± 503.77	<0.001
Age at MRI scan, wk	37.67 ± 1.94	39.91 ± 1.52	<0.001
Male	33 (37.1)	22 (51.2)	0.136
Maternal age, years	34.42 ± 4.10	33.36 ± 3.58	0.153
Maternal education, years	15.69 ± 1.59	15.77 ± 1.52	0.779

Data are presented as the mean ± SD or number (%).

Table 2
Neurodevelopmental follow-up of preterm and term infants at 18–22 month of age.

Variables	Preterm (n = 89)	Term (n = 43)	P-value
Neurodevelopmental follow-up at 18–22 month of age			
BSID III cognitive ability	97.17 ± 12.76	100.66 ± 10.85	0.144
Cognitive delay, n (%)	9/88 (10.2)	1/38 (2.6)	0.280
BSID III language ability	89.41 ± 13.42	97.16 ± 11.15	<0.001
Language delay, n (%)	36/88 (40.9)	5/38 (13.2)	0.002
Receptive scaled score	8.74 ± 2.44	9.42 ± 1.61	0.117
Expressive scaled score	8.20 ± 2.53	9.89 ± 1.54	<0.001
BSID III motor ability	96.36 ± 16.33	107.42 ± 13.25	0.001
Motor delay, n (%)	15/88 (17)	0 (0)	0.005
BSID III social-emotional ability	98.18 ± 16.54	108.68 ± 14.69 (21/33)	0.001
Social-emotional delay, n (%)	14/88 (15.9)	0 (0)	0.010

Data are presented as the mean ± SD or number (%). Delay defined as composite scores of < 85. Abbreviations: BSID, Bayley Scales of infant and Toddler Development.

3.2. Classification performance

Table 3 shows the classification performance metrics of the elastic net logistic regression model. Using the pathway atlas with a 10% threshold level, we found that the elastic net logistic regression demonstrated the highest and most significant accuracy (87.9%, $p < 0.002$). The sensitivity, specificity, f1 score, and positive predicted value of this method were 92.2%, 79.5%, 90.58%, and 90.7%, respectively. The performance of the classification model using adjusted DTI metrics in the pathway ROI with three different threshold levels (30%, 50%, and 70%), while significant, was suboptimal. Setting the threshold of the pathway atlas to 30%, 50%, and 70% yielded the following metrics of performance for the elastic net logistic regression model: A threshold of 30% yielded an accuracy of 84.9%, sensitivity of 91%, specificity of 72.5%, f1 score of 88.76%, and positive predicted value of 87.1%; 50% yielded an accuracy of 80.4%, sensitivity of 90%, specificity of 60.5%, f1 score of 86.2%, and positive predicted value of 82.6%; 70% yielded an accuracy of 84.2%, sensitivity of 93.3%, specificity of 66%, f1 score of 88.8%, and positive predicted value of 85.5%. The moderate and suboptimal classification performance metrics of the other models are presented in Supplementary Table 1. The pathway atlas threshold level was finally set to 10%, as it achieved the best classification performance.

3.3. Most contributive features

Fig. 2 shows the odds ratio of the features used in the elastic net logistic regression model. The optimum values of the odds ratio of the 104 features were 5.52 and 0.28. The feature was selected when the

Table 3
Classification performance of the elastic net logistic regression. Classification results under a range of thresholds that binarize the John Hopkins University probabilistic white-matter pathway atlas prior to feature extraction, as well as the statistically significant findings from the permutation test.

Atlas threshold level	Accuracy	Sensitivity	Specificity	F1 score	PPV	Corrected P
10%	87.9	92.2	79.5	90.58	90.7	< 0.002
30%	84.9	91.0	72.5	88.76	87.1	< 0.002
50%	80.4	90.0	60.5	86.2	82.6	< 0.002
70%	84.2	93.3	66.0	88.8	85.5	< 0.002

Data are presented as % values. Abbreviations: PPV, Positive Predicted Value.

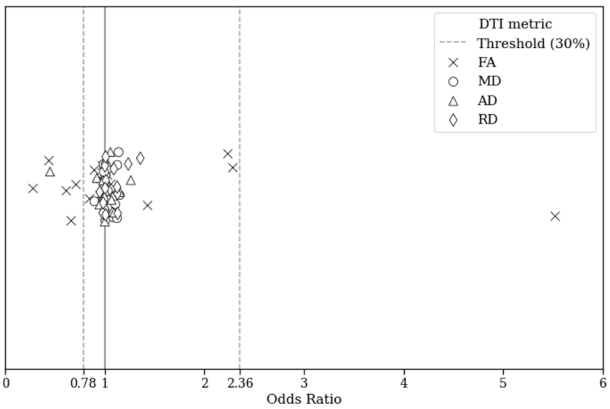

Fig. 2. Odds ratios of the elastic net logistic regression model. Dashed lines indicate the criterion that determined the most contributive features of the model. Abbreviations: FA, fractional anisotropy; MD, mean diffusivity; AD, axial diffusivity; RD, radial diffusivity.

odds ratio exceeded the given threshold of >2.36 or <0.78 (features from the baseline rather than 30% of the differences between the optimum values of odds ratio and the value of 1). Selected features consisted of the mean FA values of the body of the CC (odds ratio = 0.71), splenium of the CC (odds ratio = 0.28), middle cerebellar peduncle (MCP; odds ratio = 5.52), left and right uncinate fasciculi (odds ratio = 0.43, and 0.66, respectively), and right premotor-PMC (odds ratio = 0.61), as well as the mean AD value of the left cingulum (odds ratio = 0.45). The identified WM pathways were overlaid onto the representative FA map for each group (Fig. 3). Similar patterns were observed when other classification methods were used (Supplementary Fig. 2 and Table 4).

3.4. Correlations analysis

Pearson's correlation coefficients between the adjusted DTI metrics and neurodevelopmental outcomes were calculated for each selected feature (Table 5). Increased adjusted AD values in the left cingulum pathway were significantly correlated with the language scores after FDR correction ($r = 0.217$, $p = 0.043$). The expressive language scores showed a significant positive correlation with AD values ($r = 0.226$, $p = 0.036$). Increased adjusted AD values in the left cingulum correlated significantly with the social-emotional composite scores after FDR correction ($r = 0.31$, $p = 0.003$). Scatterplots with correlation coefficients and corresponding significances are presented in Fig. 4. Note that findings were consistent across a range of threshold levels for the pathway atlas, although there was no significant correlation between the adjusted AD values in the left cingulum and social-emotional composite scores at the 70% threshold level.

4. Discussion

The elastic net logistic regression model based on the neonatal probabilistic WM pathway revealed that preterm neonates feature an altered WM microstructure that correlates with language and social-emotional BSID-III scores. Our results thus show that a disrupted WM microstructure during preterm birth contributes to future language impairment and social-emotional problems in preterm children and confirms the potential value of using early neuroimaging markers to predict neurodevelopmental outcomes at 18–22 months of corrected age.

4.1. Importance of DTI analysis in neonates

The WM of preterm neonates during critical periods of development is more likely to undergo altered maturation and have impaired growth, than that of full-term neonates. Because the brain experiences rapid growth and elaboration of microstructural development during the neonatal period, variable myelination rates across the brain complicate feature extraction and classification in the early prediction of neurodevelopmental disorders before the onset of core symptoms (Partridge et al., 2004; Plaisier et al., 2014; Yoshida et al., 2013). WM maturation

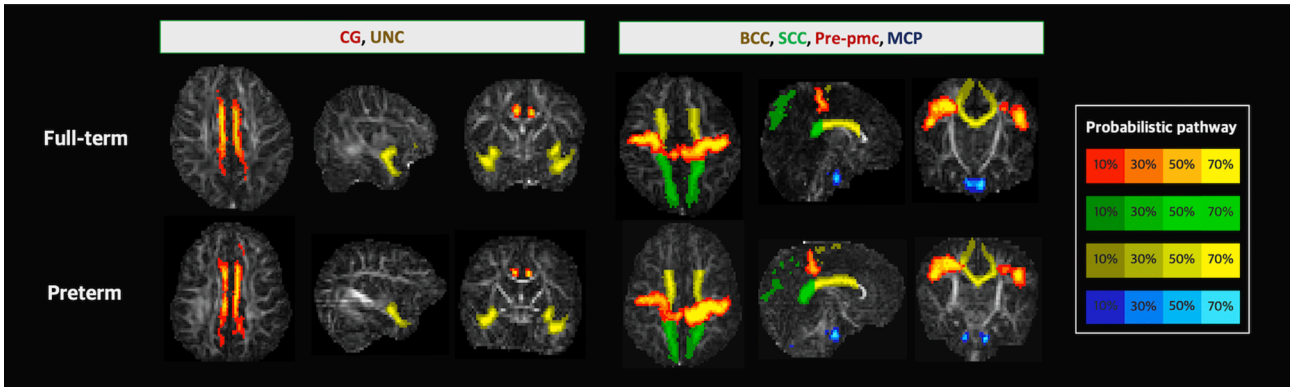

Fig. 3. Most contributive pathways identified using the elastic net logistic regression model. Most contributive features were identified and defined as alterations in the diffusion tensor imaging metrics of the specified white-matter pathways. Representative cases are illustrated for each group. Abbreviations: CG, cingulum; UNC, uncinate fasciculus; BCC, body of the corpus callosum; SCC, splenium of the corpus callosum; Pre-pmc, tract connecting the premotor and primary motor cortices; MCP, middle cerebellar peduncle.

Table 4
Features identified with other classification methods. The most contributive features were identified with LASSO logistic regression, linear kernel SVM, and random forest classification.

Pathway	Elastic net LR	LASSO LR	Linear SVM	RF
GCC				
BCC	FA		FA	
SCC	FA	FA	FA	FA, MD, RD
Cg_left	AD	AD	FA, MD, AD, RD	
Cg_right			RD	FA
CST_left			FA	FA
CST_right				AD
IFO_left			FA	
IFO_right			FA, AD	
ILF_left				
ILF_right			FA, MD, AD, RD	
MCP	FA	FA	FA	FA, MD, AD, RD
OR_left			AD	MD, RD
OR_right			FA,AD	AD
UNC_left	FA	FA	FA	MD, AD, RD
UNC_right	FA	FA	FA	MD, AD, RD
PV-V4_left				
PV-V4_right				AD
PV-MT_left				MD, AD, RD
PV-MT_right				MD, AD, RD
Pre-primaryMC_left				
Pre-primaryMC_right	FA	FA	FA	
Thal-PSC_left				
Thal-PSC_right			FA	
AR_left			FA	
AR_right			FA, MD, RD	FA

Abbreviations: FA, fractional anisotropy; MD, mean diffusivity; AD, axial diffusivity; RD, radial diffusivity; GCC, genu of the corpus callosum; BCC, body of the corpus callosum; SCC, splenium of the corpus callosum; CG, cingulum; CST, corticospinal tract; IFO, inferior fronto-occipital fasciculus; ILF, inferior longitudinal fasciculus; MCP, middle cerebellar peduncle; OR, optic radiation; UNC, uncinate fasciculus; PV-V4, tract connecting v1 + v2 and v4; PV-MT, tract connecting the v1 + v2 and MT; Pre-primaryMC, tract connecting the premotor and primary motor cortices; Thal-PSC, Tract connecting the sensory thalamus and primary sensory cortex; AR, acoustic radiation.

typically follows a posterior-to-anterior and central-to-peripheral increase in FA and decrease in MD with age (Geng et al., 2012; Rose et al., 2014). A normal trajectory of the early maturation of WM bundles includes a rapid increase in FA and decrease in MD according to various temporal and spatial patterns in the first 3 months (Dubois et al., 2008; Gao et al., 2009; Yoshida et al., 2013). In preterm infants, low FA and high MD and RD values indicate microstructural aberrations, such as low axonal fiber density and delayed myelination (Young et al., 2018). While WM AD generally increases with brain maturation and development throughout the neonatal period, abnormal WM myelination is characterized by variations in this pattern (Alexander et al., 2011).

The extraction of neuroimaging biomarkers from presymptomatic neonatal DTI data is fundamental to the early prediction of neurodevelopmental delay in the preterm population. Deficits in language processing are a major problem for preterm children, and functional and microstructural DTI studies have shown that prematurely born children and adolescents feature developmental alterations and the loss of connectivity networks, including those underlying language abilities (Myers et al., 2010; Rowlands et al., 2016). DTI provides valuable insights into the in vivo quantification of the spatiotemporal pattern of WM maturation and subtle anatomical abnormalities in pediatric populations (Pecheva et al., 2017). The region-based WM atlas was used to predict gait impairment in preterm-born toddlers with very low birth weight (Cahill-Rowley et al., 2019), investigate WM maturation in very preterm infants with and without retinopathy of prematurity (Ahn et al., 2019), and identify trajectories of early WM development in children born very preterm (Young et al., 2017). However, the pathway atlas is more suitable for the quantification of the neurodevelopmental status of the WM related to neuronal functions rather than the volumetric region-based atlas (Akazawa et al., 2016). This study used the JHU probabilistic WM pathway maps to investigate WM alterations in preterm individuals. Indeed, the presently reported statistically significant correlations between functional outcomes elucidate the consequences of preterm birth, and the utility of a probabilistic map of neonatal functional pathways in the early identification of delayed brain development.

4.2. *Prematurity-related changes in WM pathway and their clinical implications*

The present study reveals that very preterm infants at term-equivalent ages differ significantly from full-term infants in the WM pathways of the CC, MCP, uncinate fasciculi, premotor-PMC, and cingulum, suggesting widespread microstructural alterations even in the absence of detectable brain abnormalities on MRI (Lee et al., 2019). The regional microstructural vulnerability of the commissural tracts, including the CC; the projection tracts, including the MCP and premotor-PMC; and the limbic tracts, including the uncinate fasciculi and cingulum; may reflect differences in the rates and outcomes of maturation that contribute to selective vulnerability to WM injury during major subsequent changes in fetal WM (Lee et al., 2019; Rose et al., 2014). The CC and MCP appeared be most significantly and consistently affected in terms of impaired neurodevelopment, because their rapid and complex maturation during the neonatal period renders them highly sensitive to early developmental insults. Hence, despite the lack of apparent brain injury in preterm infants, their CC and cerebella feature abnormal growth trajectories relative to those in full-term infants in both adolescence and adulthood (Kontis et al., 2009; Parker et al., 2008). Northam et al. suggested that interhemispheric WM connections in the uncinate fasciculus, CC, and anterior commissure explain up to 57% of the variation in language ability among preterm-born

Table 5
Pearson correlation coefficients of the partial correlation analysis using the most contributive features.

	Language	Expressive language	Receptive language	Social-emotional	Motor	Cognition	Mean odds ratio
FA of BCC	−0.04	0.03	0.01	−0.02	−0.11	−0.1	0.71
FA of SCC	0.08	0.08	0.02	−0.01	0.03	0	0.28
FA of MCP	0.15	0.22	0.14	0.03	0.04	0.15	5.52
FA of left UNC	−0.01	0.09	−0.02	−0.11	−0.11	−0.14	0.44
FA of right UNC	0.07	0.12	0.05	0.05	−0.12	−0.11	0.66
FA of right Pre-PMC	−0.09	−0.04	−0.04	−0.06	−0.18	−0.15	0.61
AD of left CG	0.22[a]	0.23[a]	0.13	0.31[b]	0.21	0.14	0.45

Abbreviations: FA, fractional anisotropy; AD, axial diffusivity; BCC, body of the corpus callosum; SCC, splenium of the corpus callosum; MCP, middle cerebellar peduncle; UNC, uncinate fasciculus; Pre-PMC, tract connecting the premotor and primary motor cortices; CG, cingulum.
[a] FDR corrected $p < 0.05$.
[b] FDR corrected $p < 0.01$.

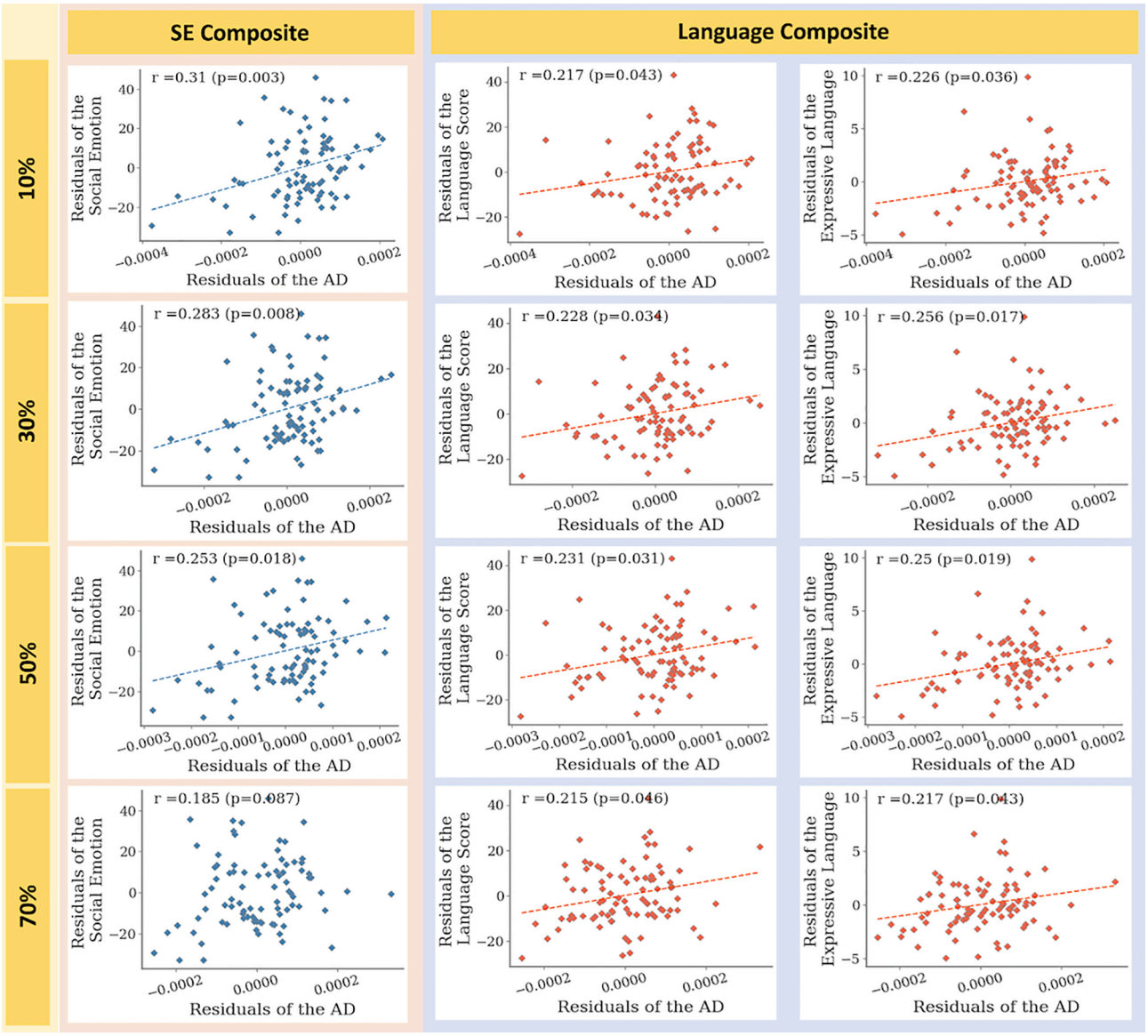

Fig. 4. Results of partial correlation. Scatter plots showing the correlation results. Each row in the figure represents a range of threshold levels defined in the binarization of the John Hopkins University (JHU) neonatal probabilistic WM pathway atlas. The columns presented the clinical developmental scores that significantly correlated with the AD values of the left cingulum. The AD values of the left cingulum and the clinical developmental scores were adjusted for post-menstrual age at scan, gestational age, and maternal education using multiple linear regression models to remove the effects of covariates. Red and blue dots indicate the very preterm individuals, and dashed lines (the linear regression results) indicate significant correlations. Abbreviations: SE Composite, social-emotional composite score; AD, axial diffusivity.

adolescents (Northam et al., 2012). Consistent with the findings of the current study, functional impairments with respect to social-emotional disorders have been reported in preterm-born children. Aberrations in the cingulum and uncinate microstructures presenting as early as at term-equivalent age may account for these findings (Rogers et al., 2018).

Our study identified an association between altered cingulum microstructure in the preterm brain at near-term age and neuro-developmental outcomes at 18–22 months of age. Impaired performance in language and social-emotional domains may involve the underlying structure of the WM pathways that connect key intra-hemispheric tracts, such as the cingulum. A functional MRI study found that cerebral regions associated with language processing were disrupted at near-term age in preterm infants who showed less interhemispheric connectivity and lateralization in the right hemisphere relative to full-term infants (Kwon et al., 2015). Although an association between the superior longitudinal fasciculus (SLF) and arcuate fasciculus (AF) WM tracts and language has been established, the roles of other WM tracts, including the uncinate and inferior longitudinal fibers, CC, and cingulum, have been identified in association with connections from the frontal to temporal lobes (Northam et al., 2012; Stipdonk et al., 2018). From term-equivalent infancy to adulthood, individuals born very preterm have been shown to exhibit smaller cingula and interconnected fornixes relative to full-term-born individuals, and a significant association has been reported between the organization of verbal information and cingulum volume (Ball et al., 2012; Caldinelli et al., 2017). Cui et al. found that lower FA of the microstructural architecture of the cingulum was associated with lower cognitive and language scores measured using the BSID-III at 12 months of age in preterm infants (Cui et al., 2017). They implicated the connections between the medial prefrontal and posterior cingulate cortices, as identified with resting-state fMRI, in the association. Preterm birth may predispose children to early onset social-emotional and behavioral problems induced by changes in

blunted cortisol reactivity and brain connectivity due to perinatal stress experienced in the neonatal intensive care unit (Provenzi et al., 2016; Scheinost et al., 2016). Notably, the cingulum was most significantly associated with behavioral impairments due to a heightened sensitivity to early developmental insults because of its rapid and complex maturation in infancy and childhood (Weinstein et al., 2011). We observed that the language abilities and social-emotional competence at 2 years of age were associated with higher AD in the left cingulum. Functional MRI data in another study showed that FA in the cingulum was inversely correlated with cognitive abilities, and RD and AD were positively associated with neurodevelopmental outcomes at 2 years of corrected age (Cui et al., 2017). In contrast, Rogers et al. scanned resting state functional connectivity in 57 very preterm infants and identified an inverse relationship between AD values from the prefrontal cortex to the cingulum and social-emotional outcomes at the age of 2 years in preterm children (Rogers et al., 2017). Furthermore, expanding upon their previous work, the investigators found that FA in the cingulum was also inversely related to social-emotional competence (Rogers et al., 2016). A few studies have investigated the relationship between aberrant and widely variable DTI measures of the WM tracts of fronto-limbic regions, including the cingulum, and the development of children with social-emotional impairment, which is a core symptom of ASD, between the ages of 2 and 4 years (Solso et al., 2016; Weinstein et al., 2011); their findings suggest that an excess of cortical neurons and early overgrowth are followed by arrested neuronal growth as well as arrested axonal and synaptic development (Solso et al., 2016; Weinstein et al., 2011).

4.3. Elastic net feature selection using DTI

Previous quantitative measurements obtained from the DTI data recorded in term- and preterm-born infants at near-term (Pannek et al., 2018), preschool (Young et al., 2018), and school ages have demonstrated group differences between specific brain regions (Murner-Lavanchy et al., 2018). However, these group-level differences focused on specific areas and the separate effects of multiple WM microstructural measures which did not allow the use of a brain-wide feature approach to identify interregional relationships between the WM microstructures (Lee et al., 2019; Murner-Lavanchy et al., 2018). Elastic net logistic regression is an excellent method with a higher classification accuracy and it does not require a large number of training samples to avoid overfitting among numerous classification models. For example, the construction of a model using soft-margin SVM with a large misclassification weight parameter may yield an optimal solution for the training set and high variance of the model. Similarly, the k-nearest neighborhood classifier with a large k results in moderately small bias but also overfitting of the training procedure. Performing classification between preterm and full-term groups with the exhaustive feature selection technique, Schadl et al. found that a number of WM alterations predicted cognitive impairment with highly explained variance (Schadl et al., 2018). Nevertheless, the exhaustive selection and classical logistic regression method usually generates a model that is overfitted to the training data set, which confounds the identification of generalized results. In contrast, the elastic net logistic regression model used in the present study considered balanced regularization and decreased the variance of the model with only a minor increase in the bias, indicating that our model offers more robust multivariate analysis.

A recent study by Girault et al. suggested that MVPA with the cross-validation of high-level features and the prediction model of linear regression can use neonatal WM connectivity to classify preterm individuals most likely to develop cognitive delay at the age of 2 with high accuracy (83.8%) (Girault et al., 2019). However, WM connections significant to cognition (a connectivity fingerprint) were identified using the deep learning model, which only classifies full-term infants according to whether they score above or below the median cognitive level. Late preterm infants (>32 weeks of gestation, >1.5 kg of birth weight) who were less likely to develop cognitive impairment were included and used for the evaluation of the model. Girault et al. did not use the DTI parameters of preterm individuals to investigate the connectivity fingerprint (Girault et al., 2019). In contrast, we hypothesized that the WM maturation of preterm individuals would differ significantly from the WM microstructures of full-term control individuals, and that the identified neural substrates may be related to subsequently evaluated neurodevelopmental domains. The accurate classification and significant correlation between the DTI alterations and subsequently recorded neurodevelopmental data support our hypothesis. Similarly, an fMRI study identified the most discriminative functional connections for the prediction of cognition deficits by using the stacked sparse autoencoder and linear-kernel SVM model (He et al., 2018). However, as fMRI data is not routinely collected from infants, the sample size for their prediction was limited. Furthermore, the marked reduction in the number of subjects might have diminished the generalizability of their results, even though the transfer learning technique was used with an independent dataset to prevent model overfitting (Raina et al., 2007; Schadl et al., 2018). Our study incorporated a relatively large dataset into the well-established regularization technique of elastic net logistic regression to investigate WM maturation in preterm infants while preventing model overfitting.

4.4. Limitations of the current study

Our study is subject to several limitations that should be addressed through future research. First, social-emotional competence was evaluated using the BSID-III social-emotional scaled scores instead of the Infant Toddler Social Emotional assessment because the latter test had not been standardized or normed for a Korean population when this study was conducted. Moreover, the reliance on the parents' report for social-emotional assessment may have resulted in the exaggeration or underestimation of their child's condition. Second, the overall size of the full-term cohort was relatively small compared to that of the preterm cohort. A follow-up study with a more balanced sample size and/or multicenter imaging data should be considered to consolidate and improve the present results before our significant findings can be generalized to larger populations. Third, the language or social-emotional scores obtained at 2 years of age may not be indicative of subsequent language impairment, as language ability and its related functional connectivity can potentially change across early childhood. Moreover, we only considered maternal education as a sociodemographic factor and disregarded others, such as household income. This may have compromised our assessment of the differential impact of WM development mediated by environmental factors on later BSID-III outcomes. Finally, as DTI sequences are typically performed with a range of b-values of 700–1500 s/mm^2, the presently used b-value of 800 s/mm^2 may not have been optimal (Duerden et al., 2019; Lean et al., 2019; Parvathaneni et al., 2018; Rose et al., 2015; Tortora et al., 2018). Earlier studies indicated that apparent diffusivity might have different resources depending on the specific b-value used, thus highlighting the need for the careful evaluation of the reproducibility of the results with a range of b-values (Hui et al., 2010).

4.5. Conclusions and future directions

We found that key structural WM regions involved in different WM substrates are characteristic of preterm infants, further suggesting the significance of altered WM in the cingulum in the development of the neonatal brain, and its capacity to reflect language organization or social-emotional skills in very preterm infants. Our results further stress that neonatal WM alterations can be used as an early biomarker for neurodevelopmental outcomes, and to facilitate more precise interventions targeting language or cognitive impairment in infants with very low birth weight during infancy. The classification models and correlation analysis presented herein may help identify specific brain regions underlying language ability at 18–22 months of age in very

preterm infants. This knowledge might aid the development of early intervention strategies and improve the developmental outcomes of affected children during their pre-symptomatic period. Future research comparing at-risk preterm children with full-term controls should be extended to include children of school age – and preferably adults – to identify specific WM substrates that may be evident in the preterm population at later periods of development. Moreover, as language skills and emotional processing require the interaction between a series of networks in the frontoparietal region of the brain (Kwon et al., 2016), future studies regarding impaired internetwork connectivity should also employ longitudinal neuroimaging and language evaluations of preterm infants. Finally, the potential of machine learning-based techniques, such as those used in the present study, warrants further development to refine predictions of individual prognoses.

CRediT authorship contribution statement

Hyun Ju Lee: Conceptualization, Resources, Data curation, Formal analysis, Writing - original draft, Visualization. **Hyeokjin Kwon:** Methodology, Software, Formal analysis, Writing - original draft, Visualization. **Johanna Inhyang Kim:** Investigation, Resources, Data curation. **Joo Young Lee:** Methodology, Formal analysis. **Ji Young Lee:** Resources, Data curation. **SungKyu Bang:** Methodology, Software. **Jong-Min Lee:** Conceptualization, Methodology, Supervision.

Declaration of Competing Interest

The authors declare that they have no known competing financial interests or personal relationships that could have appeared to influence the work reported in this paper.

Acknowledgements

This work was supported by the Bio & Medical Technology Development Program of the National Research Foundation (NRF)& funded by the Korean government (MSIT) (No. 2020M3E5D9080788), a National Research Foundation of Korea Grant funded by the Korean Government MSIT (NRF-2020-R1F1A1048529) and the research fund of Hanyang University (HY-2018).

Appendix A. Supplementary data

Supplementary data to this article can be found online at https://doi.org/10.1016/j.nicl.2020.102528.

References

Ahn, S.J., Park, H.-K., Lee, B.R., Lee, H.J., 2019. Diffusion tensor imaging analysis of white matter microstructural integrity in infants with retinopathy of prematurity. Invest. Ophthalmol. Vis. Sci. 60, 3024–3033.

Akazawa, K., Chang, L., Yamakawa, R., Hayama, S., Buchthal, S., Alicata, D., Andres, T., Castillo, D., Oishi, K., Skranes, J., 2016. Probabilistic maps of the white matter tracts with known associated functions on the neonatal brain atlas: application to evaluate longitudinal developmental trajectories in term-born and preterm-born infants. Neuroimage 128, 167–179.

Alexander, A.L., Hurley, S.A., Samsonov, A.A., Adluru, N., Hosseinbor, A.P., Mossahebi, P., Tromp, D.P., Zakszewski, E., Field, A.S., 2011. Characterization of cerebral white matter properties using quantitative magnetic resonance imaging stains. Brain Connect. 1, 423–446.

Algamal, Z.Y., Lee, M.H., 2015. Regularized logistic regression with adjusted adaptive elastic net for gene selection in high dimensional cancer classification. Comput. Biol. Med. 67, 136–145.

Avants, B.B., Epstein, C.L., Grossman, M., Gee, J.C., 2008. Symmetric diffeomorphic image registration with cross-correlation: evaluating automated labeling of elderly and neurodegenerative brain. Med. Image Anal. 12, 26–41.

Baldinger-Melich, P., Urquijo Castro, M.F., Seiger, R., Ruef, A., Dwyer, D.B., Kranz, G.S., Klöbl, M., Kambeitz, J., Kaufmann, U., Windischberger, C., 2019. Sex matters: A multivariate pattern analysis of sex-and gender-related neuroanatomical differences in cis-and transgender individuals using structural magnetic resonance imaging. Cereb. Cortex.

Ball, G., Boardman, J.P., Rueckert, D., Aljabar, P., Arichi, T., Merchant, N., Gousias, I.S., Edwards, A.D., Counsell, S.J., 2012. The effect of preterm birth on thalamic and cortical development. Cereb Cortex 22, 1016–1024.

Bayley, N. 2009. Bayley-III: Bayley Scales of infant and toddler development. Giunti OS.

Cahill-Rowley, K., Schadl, K., Vassar, R., Yeom, K., Stevenson, D.K., Rose, J., 2019. Prediction of gait impairment in toddlers born preterm from near-term brain microstructure assessed with DTI, using exhaustive feature selection and cross-validation. Front. Hum. Neurosci. 13, 305.

Caldinelli, C., Froudist-Walsh, S., Karolis, V., Tseng, C.-E., Allin, M.P., Walshe, M., Cuddy, M., Murray, R.M., Nosarti, C., 2017. White matter alterations to cingulum and fornix following very preterm birth and their relationship with cognitive functions. Neuroimage 150, 373–382.

Casanova, R., Wagner, B., Whitlow, C.T., Williamson, J.D., Shumaker, S.A., Maldjian, J. A., Espeland, M.A., 2011. High dimensional classification of structural MRI Alzheimer's disease data based on large scale regularization. Front. Neuroinf. 5, 22.

Cheong, J.L.Y., Anderson, P.J., Burnett, A.C., Roberts, G., Davis, N., Hickey, L., Carse, E., Doyle, L.W., Victorian Infant Collaborative Study, G. 2017. Changing Neurodevelopment at 8 years in children born extremely preterm since the 1990s. Pediatrics 139.

Coker-Bolt, P., Barbour, A., Moss, H., Tillman, J., Humphries, E., Ward, E., Brown, T., Jenkins, D., 2016. Correlating early motor skills to white matter abnormalities in preterm infants using diffusion tensor imaging. J. Pediatr. Rehabil. Med. 9, 185–193.

Collins, S.E., Spencer-Smith, M., Mürner-Lavanchy, I., Kelly, C.E., Pyman, P., Pascoe, L., Cheong, J., Doyle, L.W., Thompson, D.K., Anderson, P.J., 2019. White matter microstructure correlates with mathematics but not word reading performance in 13-year-old children born very preterm and full-term. NeuroImage: Clinical 24, 101944.

Cui, J., Tymofiyeva, O., Desikan, R., Flynn, T., Kim, H., Gano, D., Hess, C.P., Ferriero, D. M., Barkovich, A.J., Xu, D., 2017. Microstructure of the default mode network in preterm infants. AJNR Am. J. Neuroradiol. 38, 343–348.

Dodson, C.K., Travis, K.E., Ben-Shachar, M., Feldman, H.M., 2017. White matter microstructure of 6-year old children born preterm and full term. NeuroImage Clin. 16, 268–275.

Dubois, J., Dehaene-Lambertz, G., Perrin, M., Mangin, J.F., Cointepas, Y., Duchesnay, E., Le Bihan, D., Hertz-Pannier, L., 2008. Asynchrony of the early maturation of white matter bundles in healthy infants: quantitative landmarks revealed noninvasively by diffusion tensor imaging. Hum. Brain Mapp. 29, 14–27.

Duerden, E.G., Halani, S., Ng, K., Guo, T., Foong, J., Glass, T.J., Chau, V., Branson, H.M., Sled, J.G., Whyte, H.E., 2019. White matter injury predicts disrupted functional connectivity and microstructure in very preterm born neonates. NeuroImage Clin. 21, 101596.

Ecker, C., Marquand, A., Mourão-Miranda, J., Johnston, P., Daly, E.M., Brammer, M.J., Maltezos, S., Murphy, C.M., Robertson, D., Williams, S.C., 2010. Describing the brain in autism in five dimensions—magnetic resonance imaging-assisted diagnosis of autism spectrum disorder using a multiparameter classification approach. J. Neurosci. 30, 10612–10623.

Ecker, C., Rocha-Rego, V., Johnston, P., Mourao-Miranda, J., Marquand, A., Daly, E.M., Brammer, M.J., Murphy, C., Murphy, D.G., Consortium, M.A., 2010. Investigating the predictive value of whole-brain structural MR scans in autism: a pattern classification approach. Neuroimage 49, 44–56.

Erdei, C., Austin, N.C., Cherkerzian, S., Morris, A.R., Woodward, L.J., 2020. Predicting school-aged cognitive impairment in children born very preterm. Pediatrics 145.

Gao, W., Lin, W., Chen, Y., Gerig, G., Smith, J., Jewells, V., Gilmore, J., 2009. Temporal and spatial development of axonal maturation and myelination of white matter in the developing brain. Am. J. Neuroradiol. 30, 290–296.

Geng, X., Gouttard, S., Sharma, A., Gu, H., Styner, M., Lin, W., Gerig, G., Gilmore, J.H., 2012. Quantitative tract-based white matter development from birth to age 2years. Neuroimage 61, 542–557.

Girault, J.B., Munsell, B.C., Puechmaille, D., Goldman, B.D., Prieto, J.C., Styner, M., Gilmore, J.H., 2019. White matter connectomes at birth accurately predict cognitive abilities at age 2. Neuroimage 192, 145–155.

He, L., Li, H., Holland, S.K., Yuan, W., Altaye, M., Parikh, N.A., 2018. Early prediction of cognitive deficits in very preterm infants using functional connectome data in an artificial neural network framework. NeuroImage Clin. 18, 290–297.

Hoerl, A.E., Kennard, R.W., 1970. Ridge regression: Biased estimation for nonorthogonal problems. Technometrics 12, 55–67.

Hollund, I.M.H., Olsen, A., Skranes, J., Brubakk, A.-M., Håberg, A.K., Eikenes, L., Evensen, K.A.I., 2018. White matter alterations and their associations with motor function in young adults born preterm with very low birth weight. NeuroImage Clin. 17, 241–250.

Hui, E.S., Cheung, M.M., Chan, K.C., Wu, E.X., 2010. B-value dependence of DTI quantitation and sensitivity in detecting neural tissue changes. Neuroimage 49, 2366–2374.

Jurcoane, A., Daamen, M., Scheef, L., Bäuml, G.J., Meng, C., Wohlschläger, M.A., Sorg, C., Busch, B., Baumann, N., Wolke, D., 2016. White matter alterations of the corticospinal tract in adults born very preterm and/or with very low birth weight. Hum. Brain Mapp. 37, 289–299.

Kibria, B.M.G., 2003. Performance of some new ridge regression estimators. Commun. Statistics Simul. Comput. 32, 419–435.

Kontis, D., Catani, M., Cuddy, M., Walshe, M., Nosarti, C., Jones, D., Wyatt, J., Rifkin, L., Murray, R., Allin, M., 2009. Diffusion tensor MRI of the corpus callosum and cognitive function in adults born preterm. NeuroReport 20, 424–428.

Kwon, S.H., Scheinost, D., Lacadie, C., Sze, G., Schneider, K.C., Dai, F., Constable, R.T., Ment, L.R., 2015. Adaptive mechanisms of developing brain: cerebral lateralization in the prematurely-born. Neuroimage 108, 144–150.

Kwon, S.H., Scheinost, D., Vohr, B., Lacadie, C., Schneider, K., Dai, F., Sze, G., Constable, R.T., Ment, L.R., 2016. Functional magnetic resonance connectivity studies in infants born preterm: suggestions of proximate and long-lasting changes in language organization. Dev. Med. Child. Neurol. 58 (Suppl. 4), 28–34.
Lao, Z., Shen, D., Xue, Z., Karacali, B., Resnick, S.M., Davatzikos, C., 2004. Morphological classification of brains via high-dimensional shape transformations and machine learning methods. Neuroimage 21, 46–57.
Lean, R.E., Han, R.H., Smyser, T.A., Kenley, J.K., Shimony, J.S., Rogers, C.E., Limbrick, D.D., Smyser, C.D., 2019. Altered neonatal white and gray matter microstructure is associated with neurodevelopmental impairments in very preterm infants with high-grade brain injury. Pediatr. Res. 86, 365–374.
Lee, J.M., Choi, Y.H., Hong, J., Kim, N.Y., Kim, E.B., Lim, J.S., Kim, J.D., Park, H.K., Lee, H.J., 2019. bronchopulmonary dysplasia is associated with altered brain volumes and white matter microstructure in preterm infants. Neonatology 116, 163–170.
Li, F., Huang, X., Tang, W., Yang, Y., Li, B., Kemp, G.J., Mechelli, A., Gong, Q., 2014. Multivariate pattern analysis of DTI reveals differential white matter in individuals with obsessive-compulsive disorder. Hum. Brain Mapp. 35, 2643–2651.
Li, K., Sun, Z., Han, Y., Gao, L., Yuan, L., Zeng, D., 2015. Fractional anisotropy alterations in individuals born preterm: a diffusion tensor imaging meta-analysis. Dev. Med. Child. Neurol. 57, 328–338.
Li, Q., Xie, B., You, J., Bian, W., Tao, D., 2016. Correlated logistic model with elastic net regularization for multilabel image classification. IEEE Trans. Image Process. 25, 3801–3813.
Linsell, L., Johnson, S., Wolke, D., O'Reilly, H., Morris, J.K., Kurinczuk, J.J., Marlow, N., 2018. Cognitive trajectories from infancy to early adulthood following birth before 26 weeks of gestation: A prospective, population-based cohort study. Arch. Dis. Child 103, 363–370.
Linsell, L., Malouf, R., Morris, J., Kurinczuk, J.J., Marlow, N., 2015. Prognostic factors for poor cognitive development in children born very preterm or with very low birth weight: A systematic review. JAMA Pediatr. 169, 1162–1172.
Little, G., Beaulieu, C., 2019. Multivariate models of brain volume for identification of children and adolescents with fetal alcohol spectrum disorder. Hum. Brain Mapp.
Liu, M., Zhang, D., Shen, D., Initiative, A.s.D.N., 2012. Ensemble sparse classification of Alzheimer's disease. Neuroimage 60, 1106–1116.
Mourao-Miranda, J., Bokde, A.L., Born, C., Hampel, H., Stetter, M., 2005. Classifying brain states and determining the discriminating activation patterns: support vector machine on functional MRI data. Neuroimage 28, 980–995.
Murner-Lavanchy, I.M., Kelly, C.E., Reidy, N., Doyle, L.W., Lee, K.J., Inder, T., Thompson, D.K., Morgan, A.T., Anderson, P.J., 2018. White matter microstructure is associated with language in children born very preterm. Neuroimage Clin. 20, 808–822.
Murray, A.L., Thompson, D.K., Pascoe, L., Leemans, A., Inder, T.E., Doyle, L.W., Anderson, J.F., Anderson, P.J., 2016. White matter abnormalities and impaired attention abilities in children born very preterm. Neuroimage 124, 75–84.
Myers, E.H., Hampson, M., Vohr, B., Lacadie, C., Frost, S.J., Pugh, K.R., Katz, K.H., Schneider, K.C., Makuch, R.W., Constable, R.T., Ment, L.R., 2010. Functional connectivity to a right hemisphere language center in prematurely born adolescents. Neuroimage 51, 1445–1452.
Nichols, T.E., Holmes, A.P., 2002. Nonparametric permutation tests for functional neuroimaging: A primer with examples. Hum. Brain Mapp. 15, 1–25.
Northam, G.B., Liegeois, F., Tournier, J.D., Croft, L.J., Johns, P.N., Chong, W.K., Wyatt, J.S., Baldeweg, T., 2012. Interhemispheric temporal lobe connectivity predicts language impairment in adolescents born preterm. Brain 135, 3781–3798.
Oishi, K., Mori, S., Donohue, P.K., Ernst, T., Anderson, L., Buchthal, S., Faria, A., Jiang, H., Li, X., Miller, M.I., 2011. Multi-contrast human neonatal brain atlas: application to normal neonate development analysis. Neuroimage 56, 8–20.
Ojala, M., Garriga, G.C., 2010. Permutation tests for studying classifier performance. J. Mach. Learn. Res. 11, 1833–1863.
Pannek, K., Fripp, J., George, J.M., Fiori, S., Colditz, P.B., Boyd, R.N., Rose, S.E., 2018. Fixel-based analysis reveals alterations is brain microstructure and macrostructure of preterm-born infants at term equivalent age. Neuroimage Clin. 18, 51–59.
Parker, J., Mitchell, A., Kalpakidou, A., Walshe, M., Jung, H.Y., Nosarti, C., Santosh, P., Rifkin, L., Wyatt, J., Murray, R.M., Allin, M., 2008. Cerebellar growth and behavioural & neuropsychological outcome in preterm adolescents. Brain 131, 1344–1351.
Partridge, S.C., Mukherjee, P., Henry, R.G., Miller, S.P., Berman, J.I., Jin, H., Lu, Y., Glenn, O.A., Ferriero, D.M., Barkovich, A.J., Vigneron, D.B., 2004. Diffusion tensor imaging: serial quantitation of white matter tract maturity in premature newborns. Neuroimage 22, 1302–1314.
Parvathaneni, P., Nath, V., Blaber, J.A., Schilling, K.G., Hainline, A.E., Mojahed, E., Anderson, A.W., Landman, B.A., 2018. Empirical reproducibility, sensitivity, and optimization of acquisition protocol, for neurite orientation dispersion and density imaging using AMICO. Magn. Reson. Imaging 50, 96–109.
Pecheva, D., Yushkevich, P., Batalle, D., Hughes, E., Aljabar, P., Wurie, J., Hajnal, J.V., Edwards, A.D., Alexander, D.C., Counsell, S.J., 2017. A tract-specific approach to assessing white matter in preterm infants. Neuroimage 157, 675–694.
Pedregosa, F., Varoquaux, G., Gramfort, A., Michel, V., Thirion, B., Grisel, O., Blondel, M., Prettenhofer, P., Weiss, R., Dubourg, V., 2011. Scikit-learn: Machine learning in Python. J. Mach. Learn. Res. 12, 2825–2830.
Pereira, F., Mitchell, T., Botvinick, M., 2009. Machine learning classifiers and fMRI: A tutorial overview. Neuroimage 45, S199–S209.
Plaisier, A., Govaert, P., Lequin, M.H., Dudink, J., 2014. Optimal timing of cerebral MRI in preterm infants to predict long-term neurodevelopmental outcome: A systematic review. AJNR Am. J. Neuroradiol. 35, 841–847.
Provenzi, L., Giusti, L., Fumagalli, M., Tasca, H., Ciceri, F., Menozzi, G., Mosca, F., Morandi, F., Borgatti, R., Montirosso, R., 2016. Pain-related stress in the Neonatal Intensive Care Unit and salivary cortisol reactivity to socio-emotional stress in 3-month-old very preterm infants. Psychoneuroendocrinology 72, 161–165.
Raina, R., Battle, A., Lee, H., Packer, B., Ng, A.Y., 2007. Self-taught learning: transfer learning from unlabeled data. In: Proceedings of the 24th international conference on Machine learning, pp. 759–766.
Rajagopalan, V., Scott, J.A., Liu, M., Poskitt, K., Chau, V., Miller, S., Studholme, C., 2017. Complementary cortical gray and white matter developmental patterns in healthy, preterm neonates. Hum. Brain Mapp. 38, 4322–4336.
Rogers, C.E., Lean, R.E., Wheelock, M.D., Smyser, C.D., 2018. Aberrant structural and functional connectivity and neurodevelopmental impairment in preterm children. J. Neurodev. Disord 10, 38.
Rogers, C.E., Smyser, T., Smyser, C.D., Shimony, J., Inder, T.E., Neil, J.J., 2016. Regional white matter development in very preterm infants: perinatal predictors and early developmental outcomes. Pediatr. Res. 79, 87–95.
Rogers, C.E., Sylvester, C.M., Mintz, C., Kenley, J.K., Shimony, J.S., Barch, D.M., Smyser, C.D., 2017. Neonatal amygdala functional connectivity at rest in healthy and preterm infants and early internalizing symptoms. J. Am. Acad. Child Adolesc. Psychiatry 56, 157–166.
Rose, J., Cahill-Rowley, K., Vassar, R., Yeom, K.W., Stecher, X., Stevenson, D.K., Hintz, S. R., Barnea-Goraly, N., 2015. Neonatal brain microstructure correlates of neurodevelopment and gait in preterm children 18–22 mo of age: An MRI and DTI study. Pediatr. Res. 78, 700–708.
Rose, J., Vassar, R., Cahill-Rowley, K., Guzman, X.S., Stevenson, D.K., Barnea-Goraly, N., 2014. Brain microstructural development at near-term age in very-low-birth-weight preterm infants: An atlas-based diffusion imaging study. Neuroimage 86, 244–256.
Rowlands, M.A., Scheinost, D., Lacadie, C., Vohr, B., Li, F., Schneider, K.C., Todd Constable, R., Ment, L.R., 2016. Language at rest: A longitudinal study of intrinsic functional connectivity in preterm children. Neuroimage Clin. 11, 149–157.
Ryali, S., Supekar, K., Abrams, D.A., Menon, V., 2010. Sparse logistic regression for whole-brain classification of fMRI data. Neuroimage 51, 752–764.
Sansavini, A., Guarini, A., Justice, L.M., Savini, S., Broccoli, S., Alessandroni, R., Faldella, G., 2010. Does preterm birth increase a child's risk for language impairment? Early Human Dev. 86, 765–772.
Schadl, K., Vassar, R., Cahill-Rowley, K., Yeom, K.W., Stevenson, D.K., Rose, J., 2018. Prediction of cognitive and motor development in preterm children using exhaustive feature selection and cross-validation of near-term white matter microstructure. Neuroimage Clin. 17, 667–679.
Scheinost, D., Kwon, S.H., Lacadie, C., Sze, G., Sinha, R., Constable, R.T., Ment, L.R., 2016. Prenatal stress alters amygdala functional connectivity in preterm neonates. Neuroimage Clin. 12, 381–388.
Seabold, S., Perktold, J., 2010. Statsmodels: Econometric and statistical modeling with python. Proceedings of the 9th Python in Science Conference. Scipy, pp. 61.
Serenius, F., Ewald, U., Farooqi, A., Fellman, V., Hafstrom, M., Hellgren, K., Marsal, K., Ohlin, A., Olhager, E., Stjernqvist, K., Stromberg, B., Aden, U., Kallen, K., Extremely Preterm Infants in Sweden Study, G, 2016. Neurodevelopmental Outcomes among extremely preterm infants 6.5 years after active perinatal care in Sweden. JAMA Pediatr. 170, 954–963.
Shen, L., Kim, S., Qi, Y., Inlow, M., Swaminathan, S., Nho, K., Wan, J., Risacher, S.L., Shaw, L.M., Trojanowski, J.Q., 2011. Identifying neuroimaging and proteomic biomarkers for MCI and AD via the elastic net. In: International Workshop on Multimodal Brain Image Analysis. Springer, pp. 27–34.
Solso, S., Xu, R., Proudfoot, J., Hagler Jr., D.J., Campbell, K., Venkatraman, V., Carter Barnes, C., Ahrens-Barbeau, C., Pierce, K., Dale, A., Eyler, L., Courchesne, E., 2016. Diffusion tensor imaging provides evidence of possible axonal overconnectivity in frontal lobes in autism spectrum disorder toddlers. Biol. Psychiatry 79, 676–684.
Stipdonk, L.W., Franken, M.J.P., Dudink, J., 2018. Language outcome related to brain structures in school-aged preterm children: A systematic review. PLoS One 13, e0196607.
Stolicyn, A., Harris, M.A., Shen, X., Barbu, M.C., Adams, M.J., Hawkins, E.L., de Nooij, L., Yeung, H.W., Murray, A.D., Lawrie, S.M., 2020. Automated classification of depression from structural brain measures across two independent community-based cohorts. Hum. Brain Mapp.
Tang, Z., Liu, Z., Li, R., Yang, X., Cui, X., Wang, S., Yu, D., Li, H., Dong, E., Tian, J., 2017. Identifying the white matter impairments among ART-naïve HIV patients: a multivariate pattern analysis of DTI data. Eur. Radiol. 27, 4153–4162.
Tibshirani, R., 1996. Regression shrinkage and selection via the lasso. J. Roy. Stat. Soc. Ser. B (Methodol.) 58, 267–288.
Tortora, D., Martinetti, C., Severino, M., Uccella, S., Malova, M., Parodi, A., Brera, F., Morana, G., Ramenghi, L.A., Rossi, A., 2018. The effects of mild germinal matrix-intraventricular haemorrhage on the developmental white matter microstructure of preterm neonates: A DTI study. Eur. Radiol. 28, 1157–1166.
Tustison, N.J., Avants, B.B., Cook, P.A., Zheng, Y., Egan, A., Yushkevich, P.A., Gee, J.C., 2010. N4ITK: Improved N3 bias correction. IEEE Trans. Med. Imaging 29, 1310–1320.
Twilhaar, E.S., Wade, R.M., de Kieviet, J.F., van Goudoever, J.B., van Elburg, R.M., Oosterlaan, J., 2018. Cognitive outcomes of children born extremely or very preterm since the 1990s and associated risk factors: A meta-analysis and meta-regression. JAMA Pediatr. 172, 361–367.
Vounou, M., Nichols, T.E., Montana, G., Initiative, A.S.D.N., 2010. Discovering genetic associations with high-dimensional neuroimaging phenotypes: A sparse reduced-rank regression approach. Neuroimage 53, 1147–1159.
Weinstein, M., Ben-Sira, L., Levy, Y., Zachor, D.A., Ben Itzhak, E., Artzi, M., Tarrasch, R., Eksteine, P.M., Hendler, T., Ben Bashat, D., 2011. Abnormal white matter integrity in young children with autism. Hum. Brain Mapp. 32, 534–543.

Yang, Y., Zou, H., 2013. A cocktail algorithm for solving the elastic net penalized Cox's regression in high dimensions. Statistics Interf. 6, 167–173.
Yoshida, S., Oishi, K., Faria, A.V., Mori, S., 2013. Diffusion tensor imaging of normal brain development. Pediatr. Radiol. 43, 15–27.
Young, J.M., Morgan, B.R., Whyte, H.E., Lee, W., Smith, M.L., Raybaud, C., Shroff, M.M., Sled, J.G., Taylor, M.J., 2017. Longitudinal study of white matter development and outcomes in children born very preterm. Cereb. Cortex 27, 4094–4105.
Young, J.M., Vandewouw, M.M., Morgan, B.R., Smith, M.L., Sled, J.G., Taylor, M.J., 2018. Altered white matter development in children born very preterm. Brain Struct. Funct. 223, 2129–2141.
Zou, H., Hastie, T., 2005. Regularization and variable selection via the elastic net. J. R. Statistical Soc. Ser. B Statistical Methodol. 67, 301–320.